

# Theoretical Aspects of Liquid Crystals and Liquid Crystalline Polymers

James J. Feng

Department of Chemical and Biological Engineering and Department of Mathematics,  
University of British Columbia, Vancouver, British Columbia, Canada

## INTRODUCTION

Liquid crystallinity refers to an intermediate state of matter where the molecules exhibit a degree of order that is between that of ordinary liquids and solids. Typically, these molecules have an elongated shape and an intrinsic tendency toward alignment. Yet, the inter-molecular forces are not so strong as to bind them into a regular lattice as in crystalline solids. Thus, the orientational order among the molecules makes the material anisotropic and “crystalline,” while the lack of strong positional order allows the material to flow like ordinary fluids. This liquid–solid duality gives rise to much of the “anomalous” behavior of liquid crystalline materials. When understood, however, their unique dynamics can be harnessed to produce high-performance materials with unique properties.

In this entry, we review the state of the art in theoretical modeling and computation of the flow and rheology of low-molecular-weight liquid crystals (LCs) and liquid crystalline polymers (LCPs). The latter can be viewed as macromolecular liquid crystals, and the significance of the molecular weight will be made clear shortly. We restrict our scope to nematics, one of the several types of LCs with no positional order altogether;<sup>[1]</sup> they seem to have the most important applications and have been the focus of theoretical efforts. Owing to the long-standing academic and industrial interest in these materials, their dynamics have been summarized in several reviews, e.g., Refs.<sup>[1–4]</sup> While overlapping those in certain aspects, we emphasize constitutive modeling and numerical simulation of defects and texture. The latter nicely demonstrates the interplay between macroscopic flow and mesoscopic orientation, a hallmark of liquid crystalline dynamics. Due to space limitation, we will attempt to construct a coherent framework instead of an exhaustive literature review. Based on their conceptual origins, we discuss continuum theories and molecular theories separately. In addition, a theory for liquid crystalline materials has been proposed based on nonequilibrium thermodynamics.<sup>[5]</sup> As the theoretical framework and mathematical representation are quite independent of the other theories, we will not discuss

this theory but refer the reader to Beris and Edwards’ monograph.<sup>[5]</sup>

Because of similar molecular attributes, LCs and LCPs share enough common features to be discussed in this single entry. A significant difference is that the large LCP molecules have a much longer relaxation time. Thus, the molecular conformation of LCPs is easily disturbed by flow and deformation. Rheologically, therefore, the material exhibits “molecular viscoelasticity” as macromolecular fluids normally do. Small-molecule LCs relax so fast that their molecular configuration remains almost always at equilibrium; there is no viscoelasticity. Both LCs and LCPs resist spatial distortion to their orientational pattern. This tendency is known as “distortional elasticity.” The continuum theories were originally developed for small-molecule LCs, capturing distortional elasticity but not molecular viscoelasticity. Molecular theories, on the other hand, have evolved to contain both ingredients. Not surprisingly, a properly constructed molecular theory should reduce to a continuum theory in the limit of vanishing molecular relaxation time.

## CONTINUUM THEORIES

The tendency of LCs to resist and recover from distortion to their orientation field bears clear analogy to the tendency of elastic solids to resist and recover from distortion of their shape (strain). Based on this idea, Oseen, Zocher, and Frank established a linear theory for the distortional elasticity of LCs.<sup>[1]</sup> Ericksen<sup>[6,7]</sup> incorporated this into hydrostatic and hydrodynamic theories for nematics, which were further augmented by Leslie<sup>[8]</sup> with constitutive equations. The Leslie–Ericksen theory has been the most widely used LC flow theory to date.

### Frank Elasticity

Viewing the LC as an anisotropic continuum, a pseudo-vector  $\mathbf{n}$  of unit length, called the director, is used to indicate the orientation field. Thus, orientational

distortion is described by the spatial gradient  $\nabla \mathbf{n}(\mathbf{r})$ . Retaining quadratic terms, one may write the free energy density for orientation distortion as:<sup>[1]</sup>

$$F_d = \frac{K_1}{2} (\nabla \cdot \mathbf{n})^2 + \frac{K_2}{2} (\mathbf{n} \cdot \nabla \times \mathbf{n})^2 + \frac{K_3}{2} |\mathbf{n} \times \nabla \times \mathbf{n}|^2 \quad (1)$$

where the coefficients  $K_1$ ,  $K_2$ , and  $K_3$  are elastic constants corresponding to three canonical forms of orientational distortion: splay, twist, and bend.<sup>[1]</sup> The  $K$ 's have the dimension of force, and  $F_d$  has the dimension of energy per unit volume. When the three  $K$ 's are equal, the free energy takes on a particularly simple form:

$$F_d = \frac{K}{2} \nabla \mathbf{n} : (\nabla \mathbf{n})^T \quad (2)$$

Thus the “one-constant approximation” is often used in theoretical analysis.

### Leslie–Ericksen Theory

When  $\mathbf{n}(\mathbf{r})$  is disturbed, say by an external magnetic field, an elastic torque arises:

$$\mathbf{h} = -\frac{\delta F_d}{\delta \mathbf{n}} = -\frac{\partial F_d}{\partial \mathbf{n}} + \nabla \cdot \left( \frac{\partial F_d}{\partial \nabla \mathbf{n}} \right) \quad (3)$$

Known as the molecular field,  $\mathbf{h}$  tends to restore  $\mathbf{n}$  to its former orientation. Minimizing the total free energy shows that an equilibrium is achieved when  $\mathbf{h}$  is parallel to  $\mathbf{n}$ . Furthermore, when the LC is deformed, the variation of  $F_d(\mathbf{n}, \nabla \mathbf{n})$ , with respect to the strain, gives rise to an elastic stress known as the Ericksen stress:<sup>[1]</sup>

$$\sigma^E = -\frac{\partial F_d}{\partial (\nabla \mathbf{n})} \cdot (\nabla \mathbf{n})^T \quad (4)$$

The above two equations form the core of Ericksen's theory of LC hydrostatics.

Leslie recognized from early experiments that the anisotropy of the materials calls for multiple viscosity coefficients corresponding to different orientation of the LC relative to the flow. Combining this idea with the Ericksen theory leads to the Leslie–Ericksen (LE) theory, which comprises two elements: one describing the evolution of  $\mathbf{n}(\mathbf{r})$  in a flow field, and the other prescribing an extra stress tensor due to the evolving  $\mathbf{n}(\mathbf{r})$  field.

The evolution of  $\mathbf{n}(\mathbf{r})$  is governed by a balance between viscous and elastic torques:

$$\mathbf{h} = \gamma_1 \mathbf{N} + \gamma_2 \mathbf{D} \cdot \mathbf{n} \quad (5)$$

where  $\gamma_1$  and  $\gamma_2$  are viscosity coefficients,

$$\mathbf{N} = \frac{d\mathbf{n}}{dt} - \boldsymbol{\Omega} \cdot \mathbf{n} \quad (6)$$

is the rotation of  $\mathbf{n}$  relative to the background fluid,  $\boldsymbol{\Omega} = [(\nabla \mathbf{v})^T - \nabla \mathbf{v}]/2$  and  $\mathbf{D} = [(\nabla \mathbf{v})^T + \nabla \mathbf{v}]/2$  being the rotation and strain rate tensors. The molecular field  $\mathbf{h}$  is given by Eq. (3) in terms of  $\mathbf{n}$ . The Leslie–Ericksen stress tensor is written as

$$\sigma^{\text{LE}} = \sigma^E + \alpha_1 \mathbf{D} : \mathbf{n} \mathbf{n} \mathbf{n} \mathbf{n} + \alpha_2 \mathbf{n} \mathbf{N} + \alpha_3 \mathbf{N} \mathbf{n} + \alpha_4 \mathbf{D} + \alpha_5 \mathbf{n} \mathbf{n} \cdot \mathbf{D} + \alpha_6 \mathbf{D} \cdot \mathbf{n} \mathbf{n} \quad (7)$$

where the  $\alpha$ 's are viscosity coefficients, related to the  $\gamma$ 's of Eq. (5) by  $\gamma_1 = \alpha_3 - \alpha_2$  and  $\gamma_2 = \alpha_2 + \alpha_3 = \alpha_6 - \alpha_5$  (see Ref.<sup>[1]</sup> for explanation).

We must point out two related limitations of the LE theory. First, it applies to small-molecule LCs and to LCPs in the limit of vanishing strain rate. This is because the LE theory uses a vector  $\mathbf{n}$  to represent the orientation state of the fluid, tacitly assuming that the molecular orientation distribution stays at its equilibrium state. This is reasonable when the molecular relaxation time is much shorter than the characteristic time of the flow. Second, the theory does not allow orientational defects, which would be singularities in the  $\mathbf{n}$  field. In reality, LCs and LCPs tend to have a high density of defects.<sup>[1,9,10]</sup> Near the defect core, large spatial gradients distort the molecular orientation distribution, thus invalidating the LE theory.

### Predictions of the Leslie–Ericksen Theory for Shear Flows

The LE theory has been applied to simple shear, Poiseuille, and nonviscometric flows.<sup>[4,11]</sup> If  $\alpha_3/\alpha_2 > 0$ , the LE theory predicts a steady “flow-aligning” solution in shear flows. If  $\alpha_3/\alpha_2 < 0$ , however, no steady solution exists, and  $\mathbf{n}$  rotates continuously. The latter type, known as “tumbling” nematics, exhibits much richer dynamics. We will focus on instabilities in sheared tumbling LCs, for these reveal the most interesting physics, especially regarding the nucleation of defects. The key parameter in this problem is the Ericksen number:  $Er = \gamma_1 V H / K_1$ ,  $V$  and  $H$  being the characteristic velocity and length, respectively. It represents the interplay between the viscous torque exerted by shear and the elastic torque emanating from the wall anchoring.

Consider the shear flow geometry in Fig. 1, with three different anchoring conditions on the top and bottom planes. The initial condition is a uniform  $\mathbf{n}$  field consistent with the wall anchoring. Cases (a) and (b) are similar in which  $\mathbf{n}$  lies initially in the  $y$ - $z$  plane. In both cases, the LE theory predicts an in-plane tumbling instability and an out-of-plane twist instability.<sup>[12]</sup>

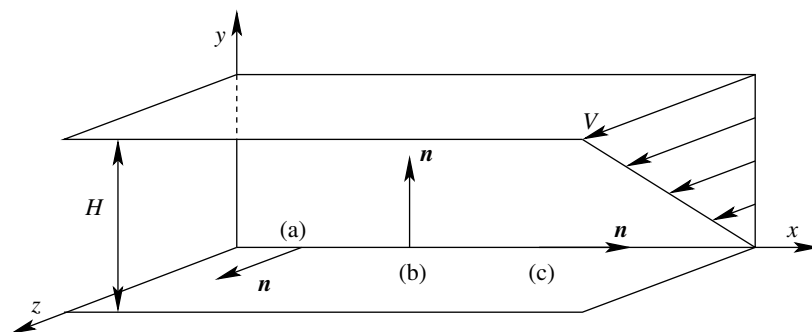


**Fig. 1** Geometry for shear flow, with three possible anchoring conditions on the top and bottom planes: (a)  $\mathbf{n}$  fixed along the flow direction (planar anchoring); (b)  $\mathbf{n}$  fixed along the velocity gradient (homeotropic anchoring); and (c)  $\mathbf{n}$  fixed along the vorticity direction (log rolling).

If  $\mathbf{n}$  is restricted to the  $y$ - $z$  plane during the shear, a steady “windup” solution obtains for low shear rates, with  $\mathbf{n}$  rotating the most at the center and less toward the walls. This windup picture becomes unstable at a critical shear rate, where the director tumbles discontinuously to a new solution with reduced elastic energy. The critical  $Er$  depends on material parameters, and falls roughly between 10 and 100. Mathematically, this instability is represented by the existence of multiple in-plane solutions at certain ranges of the shear rate.<sup>[13]</sup> An example is shown in Fig. 2.

If one relaxes the constraint of in-plane orientation, a second instability appears in roughly the same  $Er$  range, with the director being driven out of the flow-gradient ( $y$ - $z$ ) plane toward the vorticity ( $x$ ) direction.<sup>[12]</sup> This twist instability is accompanied by secondary flows orthogonal to the primary flow. Critical  $Er$  values for the tumbling and twist instabilities have been determined,<sup>[12]</sup> and detailed bifurcation diagrams constructed.<sup>[14]</sup> With increasing  $Er$ ,  $\mathbf{n}$  approaches the vorticity direction except for a thin layer next to the walls; the whole field approaches the initial condition in Fig. 1 with the anchoring condition (c).

This “log-rolling” configuration, be it the initial state with condition (c) or the result of a twist instability with conditions (a) or (b), is itself unstable to the formation of counter-rotating pairs of rolls aligned with the flow (Fig. 3A). This roll-cell instability was first recognized by linear analyses.<sup>[15,16]</sup> Along the vorticity direction, the rolls disturb the  $\mathbf{n}$  field periodically and produce alternating dark and light stripes parallel to the primary flow, which have been experimentally confirmed.<sup>[17-19]</sup>

Experiments demonstrate that at even higher  $Er$ , the rolls become unstable and irregular. Ultimately, defect lines called disclinations form in the flow direction. As the linear analysis concerns the behavior of infinitesimal disturbances, the growth of the instability and further bifurcations are inaccessible to such analyses. This motivated Feng, Tao, and Leal<sup>[20]</sup> to carry out a direct numerical simulation of a sheared nematic. Using the LE theory, with the one-constant approximation, they predicted a cascade of instabilities illustrated in Fig. 3. Steady state rolls first appear at  $Er = 2368$ . The director twists toward the flow ( $z$ ) direction at the center of the cells. With increasing  $Er$ , the secondary flow and the director twisting intensify,

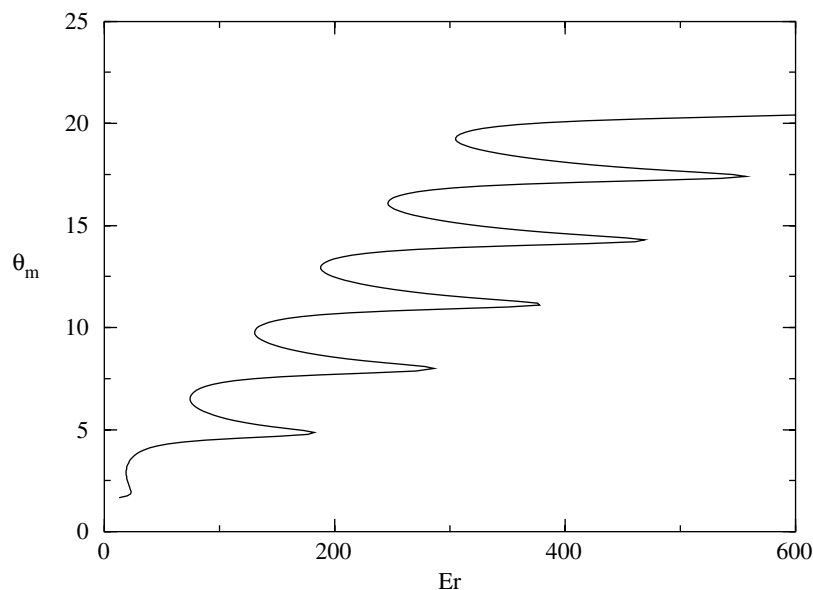


**Fig. 2** The maximum orientation angle  $\theta_m$  (in radians) as a function of  $Er$  for in-plane windup solutions of the LE theory using parameters for 8CB.<sup>[12]</sup> Multiple values of  $\theta_m$  indicate multiple solutions at one shear rate, the jumps among which are the tumbling instability.

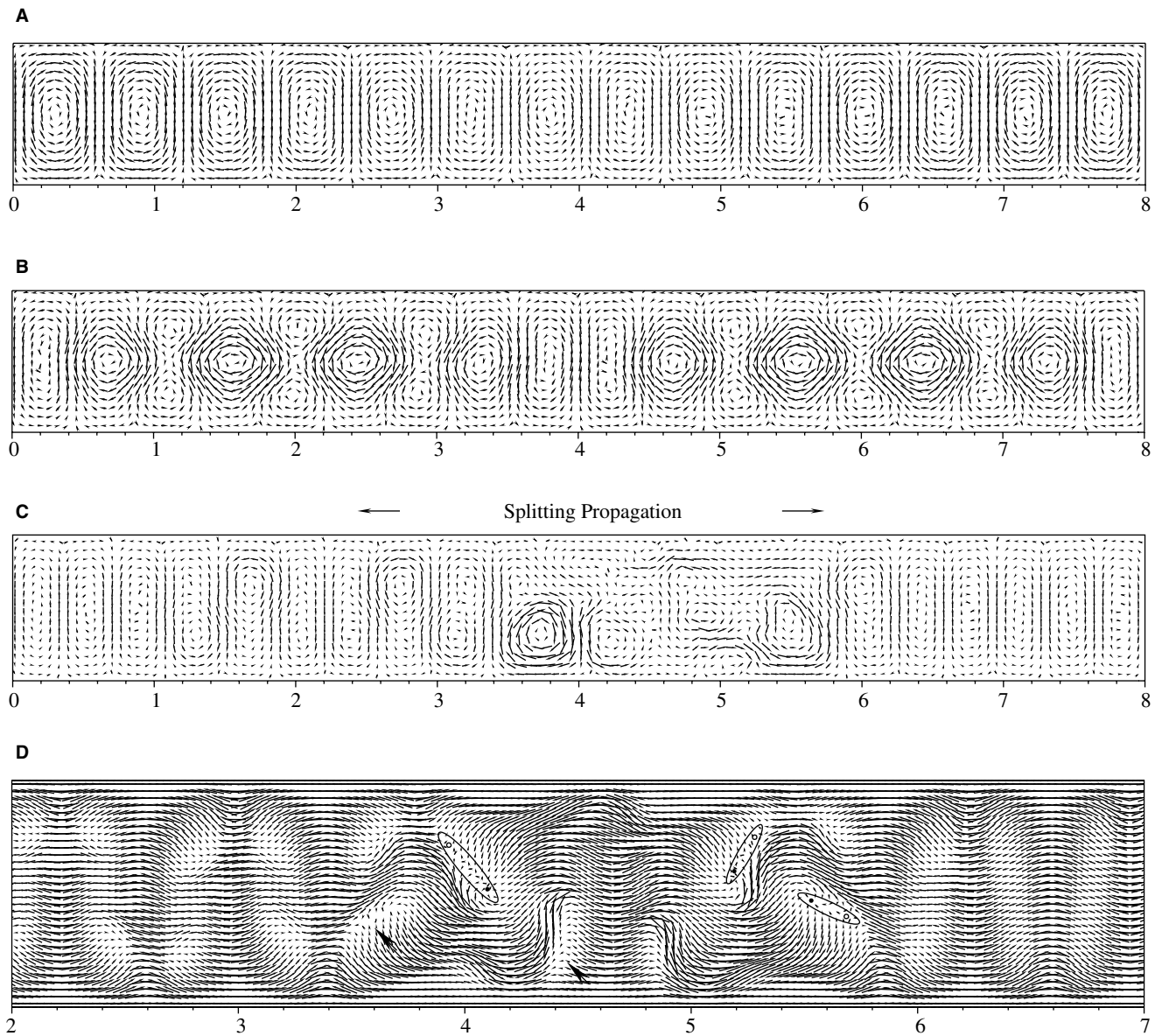


**Fig. 3** Secondary flows in the  $x$ - $y$  plane showing instabilities in a sheared nematic: (A) velocity vectors showing steady roll cells at  $Er = 2602$ ; (B) a snapshot of oscillating roll cells at  $Er = 4336$ ; (C) cell splitting at  $Er = 8672$ ; and (D) ridges, indicated by arrows, break up to produce pairs of  $\pm 1$  defects marked by the ellipses. (From Ref.<sup>[20]</sup>)

while the wavelength of the dominant mode shrinks. When  $Er$  reaches 4026, the steady solution gives way to a time-periodic one: the roll cells begin to oscillate (Fig. 3B). When  $Er$  exceeds 6867, the cells split and evolve into an irregular pattern (Fig. 3C). Meanwhile, the director field forms “ridges,” namely elongated regions where  $\mathbf{n}$  is mostly aligned with the primary flow (Fig. 3D). If the local secondary flow is favorable, the ridges break up to produce pairs of  $\pm 1$  disclinations of the escaped type with a diffuse core. This is the first detailed understanding of the process of flow-induced defect formation. More recently, Tao and Feng<sup>[21]</sup> extended this work to allow three unequal elastic

constants, and explored the interaction among the three modes of distortion during the nucleation of defects. Note that the LE theory is generally incapable of describing defects. Fortunately, the disclinations produced by broken roll cells in both experiments<sup>[18]</sup> and numerical simulations<sup>[20,21]</sup> are nonsingular lines with a diffuse core.

### Generalizations of the Leslie–Ericksen Theory

The inability of the LE theory to describe orientational defects has motivated efforts to generalize it.

The origin of the difficulty is the assumption of an equilibrium orientation distribution. In reality, the large spatial gradients at the defect would distort the molecular orientation distribution and severely reduce the local order parameter.

Ericksen<sup>[22]</sup> introduced a variable scalar order parameter; this amounts to assuming a spheroidal orientation distribution, with the axis of symmetry along the unit-length director. Liu and Walkington<sup>[23]</sup> proposed a conceptually related model by allowing the director length to vary. Its deviation from unity incurs a penalty in the Ginzburg–Landau form, and the Frank energy with the one-constant approximation can be rewritten as

$$F_{CW} = K \left[ \frac{1}{2} \nabla \mathbf{n} : (\nabla \mathbf{n})^T + \frac{(\mathbf{n} \cdot \mathbf{n} - 1)^2}{4\delta^2} \right] \quad (8)$$

The small parameter  $\delta$  indicates the extent of the defect region where  $|\mathbf{n}|$  deviates from unity; singularity is avoided as  $|\mathbf{n}|$  shrinks. Thus,  $|\mathbf{n}|$  serves the role of Ericksen's scalar parameter. Tsuji and Rey<sup>[24,25]</sup> represented the molecular orientation distribution by a second-rank tensor. Thus, the distribution is allowed an ellipsoidal shape with three distinct eigenvalues. The free energy assumes the Landau–DeGennes form.<sup>[26]</sup> Now defects correspond to points where the two largest eigenvalues are equal and a unique director cannot be defined. This theory has been used to study the appearance and evolution of spatial textures.<sup>[24,25]</sup> Finally, the Larson–Doi theory<sup>[27]</sup> is an ingenious generalization of the LE idea to a larger length scale to account for polydomain textures.

## MOLECULAR THEORIES

The starting point of a molecular constitutive theory is a simple mechanical model for the molecule that captures its most salient traits. Thus, flexible polymer molecules have been represented by elastic dumbbells and bead-spring chains,<sup>[28]</sup> and rigid polymers by rigid dumbbells<sup>[28]</sup> and rigid rods.<sup>[29]</sup> For its simplicity, the evolution of the model molecule is easily described by a convection-diffusion equation. Then a Fokker–Planck equation is written for the probability distribution function of an ensemble of these molecules. Finally, the macroscopic stress tensor is derived in terms of the distribution function. This kinetic theory framework was pioneered by Kirkwood (see, for example, Ref.<sup>[29]</sup>).

### Nematic Potentials

The orientational order in a nematic derives from inter-molecular forces of various origins. We represent

such molecular interactions by a mean-field potential energy known as the nematic potential. The Onsager and the Maier–Saupe potentials have played prominent roles in the development of the subject.

The Onsager potential is based on the excluded-volume effect among rod-like molecules.<sup>[1]</sup> Consider an ensemble of rigid rods of uniform length  $L$  and diameter  $b$ , with a number density  $\nu$  and an orientation distribution function  $\Psi(\mathbf{u})$  for the molecular orientation  $\mathbf{u}$ . For a test molecule oriented in  $\mathbf{u}$ , the effect of all the other molecules can be represented by a mean-field Onsager potential:

$$V_{ON}(\mathbf{u}) = \nu kT \int \Psi(\mathbf{u}') \beta(\mathbf{u}, \mathbf{u}') d\mathbf{u}' \quad (9)$$

where  $\beta(\mathbf{u}, \mathbf{u}') = 2bL^2 |\mathbf{u} \times \mathbf{u}'|$  represents the excluded-volume interaction between two molecules along  $\mathbf{u}$  and  $\mathbf{u}'$ ,  $k$  is the Boltzmann constant,  $T$  is temperature, and the integration is over a unit sphere representing all possible orientations.

The Maier–Saupe potential is a phenomenological model originally proposed for thermotropic small-molecule LCs.<sup>[1]</sup> It is obtained by replacing the excluded-volume interaction in Eq. (9) by

$$\beta(\mathbf{u}, \mathbf{u}') = \text{const} - \beta_1 bL^2 (\mathbf{u} \cdot \mathbf{u}')^2 \quad (10)$$

where  $\beta_1$  is a constant. Then, the Maier–Saupe nematic potential can be written as:

$$\begin{aligned} V_{MS}(\mathbf{u}) &= \text{const} - \frac{3}{2} U kT \mathbf{u} \mathbf{u} : \int \Psi(\mathbf{u}') \mathbf{u} \mathbf{u}' d\mathbf{u}' \\ &= \text{const} - \frac{3}{2} U kT \mathbf{u} \mathbf{u} : \mathbf{S}, \end{aligned} \quad (11)$$

where

$$U = \frac{2}{3} \beta_1 \nu bL^2 \quad (12)$$

is called the nematic strength, and

$$\mathbf{S} = \int \Psi(\mathbf{u}') \mathbf{u}' \mathbf{u}' d\mathbf{u}' \quad (13)$$

is the second-order moment of the orientation distribution.

With either nematic potential, the equilibrium orientation distribution  $\Psi_{\text{eq}}(\mathbf{u})$  can be computed via a self-consistency condition, and the isotropic-to-nematic transition has been analyzed in terms of nematic strength parameters.<sup>[1,29]</sup>

## Doi Theory for Monodomain LCPs: Molecular Viscoelasticity

Doi developed a dynamic theory for rigid-rod polymers using the Onsager potential.<sup>[29,30]</sup> Subsequent applications mostly used the Maier–Saupe potential for mathematical simplicity; we will illustrate Doi’s theory using the latter. Consider the evolution of the orientation distribution  $\Psi(\mathbf{u})$  for an ensemble of rods in a linear flow with a constant velocity gradient  $\nabla\mathbf{v}$ .  $\Psi(\mathbf{u})$  is assumed to be spatially uniform; the nematic is a single crystal, or “monodomain.” The conservation of probability leads to the following Fokker–Planck equation:

$$\frac{\partial\Psi}{\partial t} = -\mathfrak{R} \cdot (\mathbf{u} \times \boldsymbol{\kappa} \cdot \mathbf{u}\Psi) + D_r\mathfrak{R} \cdot \left[ \mathfrak{R}\Psi + \frac{1}{kT}\Psi\mathfrak{R}V_{MS} \right] \quad (14)$$

where the rotational operator  $\mathfrak{R} = \mathbf{u} \times (\partial/\partial\mathbf{u})$ , and  $\boldsymbol{\kappa} = (\nabla\mathbf{v})^T$ .  $D_r$  is a “pre-averaged” rotational diffusivity for the rods.<sup>[29]</sup> The nematic potential  $V_{MS}$  enters as it modifies the rotation of rods by exerting a torque  $-\mathfrak{R}V_{MS}$ . An evolution equation for the second-moment tensor  $\mathbf{S}$  follows from Eq. (14):

$$\frac{\partial\mathbf{S}}{\partial t} = -6D_r\left(\mathbf{S} - \frac{\delta}{3}\right) + 6D_rU(\mathbf{S} \cdot \mathbf{S} - \mathbf{S} : \mathbf{Q}) + \boldsymbol{\kappa} \cdot \mathbf{S} + \mathbf{S} \cdot \boldsymbol{\kappa}^T - 2\boldsymbol{\kappa} : \mathbf{Q} \quad (15)$$

where  $\mathbf{Q} = \int \mathbf{u}\mathbf{u}\mathbf{u}\mathbf{u}\Psi(\mathbf{u})d\mathbf{u}$ , and  $\delta$  is the second-rank unit tensor. An elastic stress tensor can be derived by the virtual work principle:

$$\sigma_E = 3\nu kT[\mathbf{S} - U(\mathbf{S} \cdot \mathbf{S} - \mathbf{S} : \mathbf{Q})] \quad (16)$$

In addition, a viscous stress tensor arises from viscous friction on the rods:

$$\sigma_V = \frac{\nu}{2}\zeta_r\boldsymbol{\kappa} : \mathbf{Q} \quad (17)$$

where  $\zeta_r$  is a rotational friction constant defined by Doi and Edwards.<sup>[29]</sup>

For Eqs. (15)–(17) to be a self-contained rheological theory, the fourth-order moment  $\mathbf{Q}$  has to be related to the second-moment  $\mathbf{S}$  by a closure approximation. Such a closed theory describes the LCP orientation by the second-rank tensor  $\mathbf{S}$ , and the director can be identified as the eigenvector for the largest eigenvalue. Doi<sup>[30]</sup> introduced a decoupling approximation:  $\mathbf{S} : \mathbf{Q} = \mathbf{S} : \mathbf{S}\mathbf{S}$ , which turns out to be unsatisfactory as it artificially suppresses director tumbling.<sup>[31]</sup> More sophisticated closure models have since appeared, and their impact on the theory’s prediction has been

carefully examined (for example, Refs.<sup>[32,33]</sup>.) The best closure models to date preserve most of the qualitative features of the theory.

The Doi theory captures the molecular viscoelasticity of LCP, i.e., the relaxation of the orientation distribution under flow. But it completely ignores distortional elasticity and is limited to monodomains. The assumption of spatial uniformity underlies all its key elements: the nematic potential, the kinetic equation, and the elastic stress tensor. Therefore, its successes are restricted to situations where distortional elasticity is insignificant.

One such success is the prediction of anomalous normal stress differences in shear flow. Measurements indicate that the normal stress differences  $N_1$  and  $N_2$  undergo two sign changes as the shear rate increases. For small and large shear rates,  $N_1 > 0$ ,  $N_2 < 0$  as expected of flexible polymers. In an intermediate range, however,  $N_1 < 0$ ,  $N_2 > 0$ .<sup>[34]</sup> When Eq. (14) is solved without closure approximations, the Doi theory predicts three regimes of director dynamics with increasing shear rate: tumbling, wagging, and steady alignment.<sup>[31,35,36]</sup> The first sign change occurs within the tumbling regime, while the second occurs in the steady alignment regime. These transitions are linked to the spreading or narrowing of the orientation distribution  $\Psi$ . For  $N_1$  and  $N_2$ , quantitative agreement has been achieved between prediction and measurements.<sup>[34]</sup> Using the closure-approximated Doi theory, Feng and Leal<sup>[37]</sup> simulated inhomogeneous LCP flows, and showed that director tumbling can lead to defect-like patterns. They also predicted a flow-orientation instability resembling experimental observations in channel flows.<sup>[38]</sup>

## Complete Theories with Molecular Viscoelasticity and Distortional Elasticity

To add distortional elasticity to the Doi theory, one has to start with a more general nematic potential that accounts for spatial gradients. Marrucci and Greco<sup>[39]</sup> derived such a potential for nonlocal interaction among rigid-rod molecules in a distorted nematic material. For a test molecule oriented along  $\mathbf{u}$  at position  $\mathbf{r}$ , Marrucci and Greco delineated an interaction region  $V$  enveloping the test molecule. Spatial averaging of the molecular interaction inside a spherical  $V$  produces a nonlocal nematic potential:

$$V_{MG}(\mathbf{u}) = \text{const} - \frac{3}{2}UkT\left(\mathbf{S} + \frac{\Lambda^2}{24}\nabla^2\mathbf{S}\right) : \mathbf{u}\mathbf{u} \quad (18)$$

where the interaction length  $\Lambda \sim V^{1/3}$  is the only free parameter in the theory. Eq. (18) is a molecularly-based generalization of the Maier–Saupe potential.

Following the procedure in deriving the Doi theory, one arrives at a kinetic equation for  $\mathbf{S}$ :<sup>[40,41]</sup>

$$\begin{aligned} \frac{\partial \mathbf{S}}{\partial t} + \mathbf{v} \cdot \nabla \mathbf{S} &= -6D_r \left( \mathbf{S} - \frac{\delta}{3} \right) + 6D_r U (\mathbf{S} \cdot \mathbf{S} - \mathbf{S} : \mathbf{Q}) \\ &+ \boldsymbol{\kappa} \cdot \mathbf{S} + \mathbf{S} \cdot \boldsymbol{\kappa}^T - 2\boldsymbol{\kappa} : \mathbf{Q} + \frac{D_r U \Lambda^2}{8} \\ &\times (\nabla^2 \mathbf{S} \cdot \mathbf{S} + \mathbf{S} \cdot \nabla^2 \mathbf{S} - 2\nabla^2 \mathbf{S} : \mathbf{Q}) \end{aligned} \quad (19)$$

where the last line represents the consequences of the spatial gradients. Derivation of the elastic stress tensor involves subtleties in treating the nonlocal interaction among molecules. Feng, Sgalari, and Leal<sup>[41]</sup> generalized the virtual work principle to cover a finite volume of the LCP, and imposed a condition of zero work on the boundary. This leads to an elastic stress tensor:

$$\begin{aligned} \sigma_E &= 3\nu kT [\mathbf{S} - U(\mathbf{S} \cdot \mathbf{S} - \mathbf{S} : \mathbf{Q})] - \frac{\nu kT U \Lambda^2}{8} \\ &\times \left( \mathbf{S} \cdot \nabla^2 \mathbf{S} - \nabla^2 \mathbf{S} : \mathbf{Q} + \frac{\mathbf{P} - \nabla \nabla \mathbf{S} : \mathbf{S}}{4} \right) \end{aligned} \quad (20)$$

where  $P_{ij} = (\partial S_{kl} / \partial x_i)(\partial S_{lk} / \partial x_j)$ . With a proper closure approximation, Eqs. (19) and (20) constitute a “complete” constitutive theory for LCPs that incorporates both molecular viscoelasticity and distortional elasticity.

This theory has two notable features. The nonlocality of molecular interaction is reflected by the ellipticity of Eq. (19) [cf. Eq. (15)]. Thus, the LCP configuration is globally coupled by distortional elasticity. In addition, the elastic stress tensor is asymmetric. The mean-field torque on LCP molecules amounts to a “volume torque” on the material, which modifies the usual conservation of angular momentum. The antisymmetric part of the stress tensor precisely balances the volume torque computed by averaging the molecular torque.<sup>[41]</sup>

Eq. (18) is actually a special form of the Marrucci–Greco potential obtained by taking a spherical interaction region around a test molecule. This corresponds, in the limit of weak distortion, to the one-constant approximation in Frank elasticity. Accounting for the molecular length in an oblong interaction region, Marrucci and Greco<sup>[39]</sup> derived a more general potential that produces three unequal elastic constants. Wang<sup>[42]</sup> has built this general nematic potential into a dynamic theory. Finally, we note several alternatives to the kinetic approach of LCP rheology.<sup>[5,24,43]</sup> Despite the different starting points, the complete theories obtained are essentially the same.

## Predictions of the Complete Theories

As the complete theories include both molecular viscoelasticity and distortional elasticity, an outstanding question is: do they predict the correct dynamics for texture evolution that have eluded previous simpler models? So far, efforts to answer this have been limited to numerical simulations on shear flows.

Kupferman, Kawaguchi, and Denn<sup>[40]</sup> assumed no streamwise (along  $z$  in Fig. 1) or spanwise (along  $x$ ) variations and a two-dimensional orientation with all molecules lying on the  $y$ – $z$  plane. A one-dimensional “windup” picture emerges, similar to the Leslie–Erickson predictions.<sup>[13]</sup> At low shear rates, a steady state is reached. At higher shear rates, the director continues to tumble in the interior of the domain, with the near-wall distortion being released periodically. A disappointing feature of the result is the lack of an inherent texture length scale that would reflect the balance between elastic and viscous torques.<sup>[3]</sup>

Rey and Tsuji<sup>[24,25]</sup> permitted two-dimensional variations of orientation on the  $y$ – $z$  plane, but decoupled the flow field from the kinetic equation so that the linear velocity profile is fixed and unperturbed by LCP stress. Results reveal the conflict between the tumbling tendency far from the anchoring walls and the fixed orientation at the walls, which is resolved by periodic nucleation of a pair of defects. Again, no inherent texture length scale emerges. The common features of the above solutions—a windup structure and periodic appearance and annihilation of  $\pm 1/2$  defects—are similar to the prediction of the original Doi theory.<sup>[32,37,38]</sup> Thus, a key expectation of the complete theories, namely the prediction of a texture length independent of macroscopic geometry, is not fulfilled, perhaps owing to the simplifications in these simulations.

Sgalari, Leal, and Feng<sup>[44]</sup> sought to relax the geometric and physical restrictions in simulating shear flows. The constitutive and momentum equations are fully coupled, with the flow affecting the LCP orientation, and the resulting stress tensor modifying the flow in return. Two-dimensional variations on the  $y$ – $z$  plane are allowed, though the configuration tensor  $\mathbf{S}$  is assumed to be symmetric about the shear plane as in Tsuji and Rey.<sup>[24]</sup> Finally, the dependence of the rotational diffusivity on the order parameter, the so-called tube dilation effect,<sup>[29]</sup> is included. Upon startup of shear, the interior of the domain tumbles as seen before. In time, however, this tumbling is arrested by distortional elasticity, and narrow strips containing much-reduced order emerge along the flow direction. These strips are roughly parallel to each other and are taken to be disclination lines. A characteristic texture length  $h_{\text{text}}$  is identified from the Fourier spectrum of the order parameter profiles.  $h_{\text{text}}$  refines in time and approaches an equilibrium level in about 100 strain

units (Fig. 4A). Marrucci's argument for the inherent texture length,<sup>[3]</sup> carried over to the complete molecular theory, yields the following scaling:

$$h_{\text{text}} \propto \Lambda \left( \frac{U}{De} \right)^{1/2} \quad (21)$$

where  $De$  is the Deborah number of the flow. The numerical data appear to be consistent with the square-root scaling (Fig. 4B). Sgalari, Leal, and Feng<sup>[44]</sup> further removed the restriction on  $\mathbf{S}$  being symmetric about the shear plane. Then, the complete theory predicts an out-of-plane twist instability resembling the predictions of the LE theory.<sup>[12]</sup>

More recently, Sgalari, Leal, and Meiberg<sup>[45]</sup> and Klein and Leal<sup>[46]</sup> examined the instability of simple shear to secondary flows in the  $x$ - $y$  plane. The initial instability takes on a similar form to that predicted by the LE theory, with the appearance and subsequent

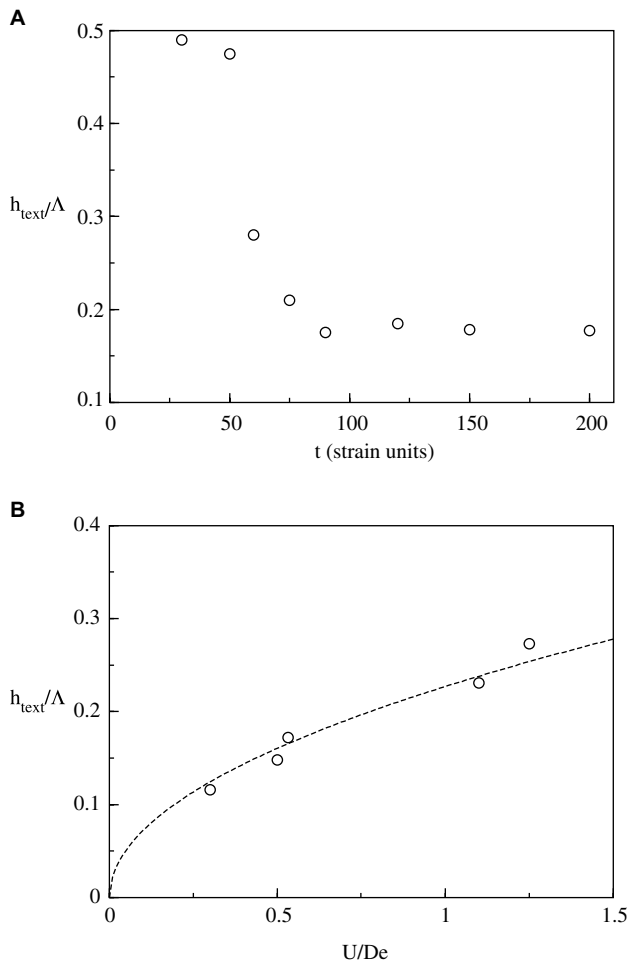


**Fig. 4** (A) Evolution of  $h_{\text{text}}$  in time for  $U = 8$ ,  $De = 15$ ,  $Er = 8 \times 10^6$ ,  $\Lambda/H = 10^{-3}$  and (B) scaling for  $h_{\text{text}}$  when  $U/De$  is varied. The data points are numerical results and the dotted line indicates the square-root law of Eq. (21). (From Ref.<sup>[44]</sup>.)

breakup of roll cells.<sup>[20]</sup> But the complete theory allows these authors to probe director turbulence and the Deborah-number cascade at much higher shear rates.<sup>[18]</sup> The authors argued that  $\pm 1/2$  strength “thin” defects would eventually appear in addition to the escaped  $\pm 1$  disclinations noted before.

### Connection Between Molecular and Continuum Theories

As alluded to in the introduction to this entry, the LE theory was conceived for small molecule LCs while molecular theories are intended for LCPs. LC molecules retain their equilibrium orientation distribution. LCPs are susceptible to disturbances to their distribution function  $\Psi(\mathbf{u})$ ; its temporal relaxation gives rise to molecular viscoelasticity, while its spatial gradient produces distortional elasticity. A natural question is whether the molecular theories reduce properly to the continuum LE theory in the limiting case of an undisturbed orientation distribution. This situation arises in the “weak flow limit” where the flow is weak ( $De \ll 1$ ) and spatial distortions are small ( $|\nabla \mathbf{S}| \ll 1/\Lambda$ ). In this limit, Feng, Sgalari, and Leal<sup>[41]</sup> has proved that their version of the complete theory reduces properly to the LE theory.

Their proof relies on the fact that in the limit of small spatial distortions, The Marrucci–Greco potential of Eq. (18) reduces to the Frank elastic energy of Eq. (2) with

$$K = \frac{1}{8} \nu k T U S_{\text{eq}}^2 \Lambda^2 \quad (22)$$

$S_{\text{eq}}$  being the equilibrium order parameter. Feng, Sgalari, and Leal<sup>[41]</sup> followed the unusual perturbation procedure outlined by Kuzuu and Doi,<sup>[47]</sup> in which the base state is undetermined because a uniform single crystal does not have a preferred orientation. The kinetic equation and stress tensor reduce precisely to the LE forms, with the phenomenological elastic and viscous constants determined by equilibrium molecular parameters.

As indicated above, such an agreement is perhaps expected. On the other hand, it is remarkable that a rather complex phenomenological theory postulated for an LC continuum can be reconciled with an even more complex molecular theory built on the concept of intermolecular potential. Perhaps the only other such happy instance is the agreement between the continuum Oldroyd-B model for viscoelastic liquids and the molecular model based on a dilute suspension of linear Hookean dumbbells in a Newtonian solvent.<sup>[28]</sup>

The idea that the LE theory applies to weak flows, while the molecular theories to strong flows provides a convenient framework for interpreting experimental

observations. Larson and Mead<sup>[18]</sup> identified the so-called Ericksen number ( $Er$ ) and the Deborah number ( $De$ ) cascades for sheared nematic polymers. At lower shear rates, the molecular distribution remains largely undisturbed although the preferred orientation—the director—rotates. The dynamics are thus dictated by  $Er$ , the ratio between viscous and distortional elastic effects. The LE simulations of Feng, Tao, and Leal<sup>[20]</sup> and Tao and Feng<sup>[21]</sup> fall in this cascade, and their results indeed correlate well to observations in the  $Er$  cascade. Higher flow rates start to distort the molecular distribution, and molecular viscoelasticity becomes significant once  $De$  rises to  $O(1)$ .<sup>[18]</sup> This is the  $De$  cascade, where distortional elasticity no longer has a major effect on certain macroscopic properties such as rheology. That is why the original Doi theory, with distortional elasticity omitted entirely, is able to reproduce the anomalous normal stress differences to quantitative accuracy.<sup>[34]</sup> For other features such as defect generation, distortional elasticity remains locally important. This is the case for the simulations of Sgalari et al.<sup>[44,45]</sup> and Klein and Leal.<sup>[46]</sup>

## CONCLUSIONS

In this brief review, we strive to construct a coherent picture of our current theoretical understanding of the flow and rheology of small-molecule and polymeric nematic liquid crystals. Owing to space limitations, we have presented results selectively, based more on the need to tell a somewhat coherent story than the significance of the work.

To sum up, there have been two types of constitutive theories for LCs and LCPs: one based on phenomenological modeling that treats the material as a continuum, and the other based on a molecular picture and a statistico-mechanical approach. The molecular theories contain the continuum LE theory as a limiting case for weak flows and small spatial distortions. Shear-flow simulations using the LE theory capture qualitative features of the Ericksen number cascade, including shear-induced defect formation. More recent simulations using a complete molecular theory have reproduced some experimental observations at higher shear rates extending into the Deborah number cascades. In particular, an inherent texture length emerges and follows a scaling expected from balancing the viscous and elastic effects.

## ACKNOWLEDGMENTS

Acknowledgment is made to the Donors of The Petroleum Research Fund, administered by the American Chemical Society, for partial support. This

work was also supported by grants from the US-NSF (CTS-0229298; CTS-9984402), the NSERC and the Canada Research Chair program and the NNSF of China (No. 20174024 and No. 20490220).

## REFERENCES

- de Gennes, P.G.; Prost, J. *The Physics of Liquid Crystals*, 2nd Ed.; Oxford University Press: New York, 1993.
- Larson, R.G. *The Structure and Rheology of Complex Fluids*; Oxford University Press: New York, 1999.
- Marrucci, G.; Greco, F. Flow behavior of liquid crystalline polymers. *Adv. Chem. Phys.* **1993**, *86*, 331–404.
- Rey, A.D.; Denn, M.M. Dynamical phenomena in liquid–crystalline materials. *Ann. Rev. Fluid Mech.* **2002**, *34*, 233–266.
- Beris, A.N.; Edwards, B.J. *Thermodynamics of Flowing Systems with Internal Microstructure*; Oxford University Press: New York, 1994.
- Ericksen, J.L. Hydrostatic theory of liquid crystals. *Arch. Rational Mech. Anal.* **1962**, *9*, 371–378.
- Ericksen, J.L. On equations of motion for liquid crystals. *Quart. J. Mech. Appl. Math.* **1976**, *29* (2), 203–208.
- Leslie, F.M. Some constitutive equations for liquid crystals. *Arch. Rational Mech. Anal.* **1968**, *28*, 265–283.
- Kleman, M. Defects in liquid–crystalline polymers. *MRS Bull.* **1995**, *20* (9), 23–28.
- O'Rourke, M.J.E.; Thomas, E.L. Morphology and dynamic interaction of defects in polymer liquid crystals. *MRS Bull.* **1995**, *20* (9), 29–36.
- Chandrasekhar, S. *Liquid Crystals*, 2nd Ed.; Cambridge University Press: New York, 1992.
- Zuniga, I.; Leslie, F.M. Shear-flow instabilities in non-flow-aligning nematic liquid crystals. *Liq. Cryst.* **1989**, *5*, 725–734.
- Carlsson, T. Theoretical investigation of the shear flow of nematic liquid crystals with the Leslie viscosity  $\alpha_3 > 0$ : hydrodynamic analogue of first order phase transition. *Mol. Cryst. Liq. Cryst.* **1984**, *104*, 307–334.
- Han, W.H.; Rey, A.D. Dynamic simulations of shear-flow-induced chirality and twisted-texture transitions of a liquid–crystalline polymer. *Phys. Rev. E.* **1994**, *49*, 597–613.
- Manneville, P.; Dubois-Violette, E. Shear flow instability in sheared nematic liquids: theory steady simple shear flows. *J. Phys. Paris* **1976**, *37*, 285–296.
- Larson, R.G. Roll-cell instabilities in shearing flows of nematic polymers. *J. Rheol.* **1993**, *37*, 175–197.

17. Larson, R.G.; Mead, D.W. Development of orientation and texture during shearing of liquid-crystalline polymers. *Liq. Cryst.* **1992**, *12*, 751–768.
18. Larson, R.G.; Mead, D.W. The Ericksen number and Deborah number cascades in sheared polymeric nematics. *Liq. Cryst.* **1993**, *15*, 151–169; Corrigendum **1996**, *20*, 265.
19. Mather, P.T.; Pearson, D.S.; Larson, R.G. Flow patterns and disclination-density measurements in sheared nematic liquid crystals. II. Tumbling 8CB. *Liq. Cryst.* **1996**, *20*, 527–538.
20. Feng, J.J.; Tao, J.; Leal, L.G. Roll cells and disclinations in sheared nematic polymer. *J. Fluid Mech.* **2001**, *449*, 179–200.
21. Tao, J.; Feng, J.J. Effects of elastic anisotropy on the flow and orientation of sheared nematic liquid crystals. *J. Rheol.* **2003**, *47* (4), 1051–1070.
22. Ericksen, J.L. Liquid crystals with variable degree of orientation. *Arch. Rational Mech. Anal.* **1991**, *113*, 97–120.
23. Liu, C.; Walkington, N.J. Approximation of liquid crystal flows. *SIAM J. Numer. Anal.* **2000**, *37*, 725–741.
24. Tsuji, T.; Rey, A.D. Effect of long range order on sheared liquid crystalline materials. Part I: compatibility between tumbling behavior and fixed anchoring. *J. Non-Newton. Fluid Mech.* **1997**, *73*, 127–152.
25. Rey, A.D.; Tsuji, T. Recent advances in theoretical liquid crystal rheology. *Macromol. Theory Simul.* **1998**, *7*, 623–639.
26. De Gennes, P.G. Phenomenology of short-range-order effects in the isotropic phase of nematic materials. *Phys. Lett.* **1969**, *35A*, 454–455.
27. Larson, R.G.; Doi, M. Mesoscopic domain theory for textured liquid-crystalline polymers. *J. Rheol.* **1991**, *35*, 539–563.
28. Bird, R.B.; Curtis, C.F.; Armstrong, R.C.; Hassager, O. *Dynamics of Polymeric Liquids. Vol. 2. Kinetic Theory*; Wiley: New York, 1987.
29. Doi, M.; Edwards, S.F. *The Theory of Polymer Dynamics*; Oxford University Press: New York, 1986.
30. Doi, M. Molecular dynamics and rheological properties of concentrated solutions of rodlike polymers in isotropic and liquid crystalline phases. *J. Polym. Sci. Polym. Phys. Edn.* **1981**, *19*, 229–243.
31. Larson, R.G. Arrested tumbling in shearing flows of liquid crystal polymers. *Macromolecules* **1990**, *23*, 3983–3992.
32. Feng, J.; Chaubal, C.V.; Leal, L.G. Closure approximations for the Doi theory: which to use in simulating complex flows of liquid-crystalline polymers? *J. Rheol.* **1998**, *42*, 1095–1119.
33. Grosso, M.; Maffettone, P.L.; Halin, P.; Keunings, R.; Legat, V. Flow of nematic polymers in eccentric cylinder geometry: influence of closure approximations. *J. Non-Newton. Fluid Mech.* **2000**, *94* (2–3), 119–134.
34. Magda, J.J.; Baek, S.G.; DeVries, K.L.; Larson, R.G. Shear flows of liquid crystal polymers: measurements of the second normal stress difference and the Doi molecular theory. *Macromolecules* **1991**, *24*, 4460–4468.
35. Marrucci, G.; Maffettone, P.L. Description of the liquid-crystalline phase of rodlike polymers at high shear rates. *Macromolecules* **1989**, *22*, 4076–4082.
36. Suen, J.K.; Nayak, R.; Armstrong, R.C.; Brown, R.A. A wavelet-Galerkin method for simulating the Doi model with orientation-dependent rotational diffusivity. *J. Non-Newton. Fluid Mech.* **2003**, *114* (2–3), 197–228.
37. Feng, J.; Leal, L.G. Simulating complex flows of liquid-crystalline polymers using the Doi theory. *J. Rheol.* **1997**, *41*, 1317–1335.
38. Feng, J.; Leal, L.G. Pressure-driven channel flows of a model liquid-crystalline polymer. *Phys. Fluids* **1999**, *11*, 2821–2835.
39. Marrucci, G.; Greco, F. The elastic constants of Maier-Saupe rodlike molecule nematics. *Mol. Cryst. Liq. Cryst.* **1991**, *206*, 17–30.
40. Kupferman, R.; Kawaguchi, M.N.; Denn, M.M. Emergence of structure in a model of liquid crystalline polymers with elastic coupling. *J. Non-Newton. Fluid Mech.* **2000**, *91*, 255–271.
41. Feng, J.J.; Sgalari, G.; Leal, L.G. A theory for flowing nematic polymers with orientational distortion. *J. Rheol.* **2000**, *44* (5), 1085–1101.
42. Wang, Q. A hydrodynamic theory for solutions of nonhomogeneous nematic liquid crystalline polymers of different configurations. *J. Chem. Phys.* **2002**, *116* (20), 9120–9136.
43. Lhuillier, D. Thermo-mechanical modelling of nematic polymers. In *Continuum Thermodynamics*; Maugin, G.A., Drouot, R., Sidoroff, F.S., Eds.; Kluwer: Dordrecht, 2000; 237–246.
44. Sgalari, G.; Leal, L.G.; Feng, J.J. The shear flow behavior of LCPs based on a generalized Doi model with distortional elasticity. *J. Non-Newton. Fluid Mech.* **2002**, *102*, 361–382.
45. Sgalari, G.; Leal, L.G.; Meiberg, E. Texture evolution of sheared liquid crystalline polymers: numerical predictions of roll-cells instability, director turbulence, and striped texture with a molecular model. *J. Rheol.* **2003**, *47* (6), 1417–1444.
46. Klein, D.H.; Leal, L.G. Computational studies of the shear flow behavior of models for liquid crystalline polymers. AICHE Annual Meeting, San Francisco, November 16–21, 2003.
47. Kuzuu, N.; Doi, M. Constitutive equation for nematic liquid crystals under weak velocity gradient derived from a molecular kinetic equation. *J. Phys. Soc. Japan* **1983**, *52*, 3486–3494.